NANO LETTERS

2007
Vol. 7, No. 1
204−210

Ballistic Transport in Graphene Nanostrips in the Presence of Disorder: Importance of Edge Effects

Denis A. Areshkin,[†] Daniel Gunlycke,[‡] and Carter T. White*[,‡]

George Washington University, Washington, DC 20052, Naval Research Laboratory, Washington, DC 20375

Received September 8, 2006; Revised Manuscript Received November 8, 2006

ABSTRACT

Stimulated by recent advances in isolating graphene and similarities to single-wall carbon nanotubes, simulations were performed to assess the effects of static disorder on the conductance of metallic armchair- and zigzag-edge graphene nanostrips. Both strip types were found to have outstanding ballistic transport properties in the presence of a substrate-induced disorder. However, only the zigzag-edge strips retain these properties in the presence of irregular edges, making them better initial synthetic targets for ballistic device applications.

Novoselov, Geim, and co-workers recently succeeded in isolating macroscopic single sheets of graphite known as graphene, which they found were stable, highly crystalline, and chemically inert under ambient conditions.[1] This advance was soon followed by detailed measurements showing that these 2D sheets exhibit unusual properties such as a high-integer quantum Hall effect.[2,3] These and other experimental developments have moved us closer to graphene-based nanoelectronics, with components or even entire circuits formed from a graphene sheet.[4] However, before such a goal can be met, reliable techniques will have to be developed to selectively pattern these sheets into suitable components (either interconnected or isolated), and much analysis will be required to suggest possible targets and methods. For example, high-aspect-ratio graphene strips[5,6] with widths between 5 and 10 nm and edges terminated by σ bonds to H atoms might provide important components in carbon-based quantum electronics because they have structures suitable for in-plane device processing and electronic properties[5,6] similar to single-wall carbon nanotubes (SWNTs). However, in comparison to SWNTs, such strips, which can be viewed as cut from graphene, will probably experience a higher degree of interaction with the substrate. Also, any strips initially made are likely to have irregular edges. Stimulated by these observations and recent advances in isolating graphene, simulations were performed to assess the effects of substrate-induced and edge disorder on the conductance of metallic armchair- and zigzag-edge graphene nanostrips (GNSs). We find that, like the SWNTs,[7−11] both strip types have outstanding ballistic transport properties in the presence of a substrate-induced disorder, but only the zigzag-edge strips retain these properties in the presence of irregular edges. Our results imply that zigzag-edge GNSs are better initial synthetic targets for ballistic device applications.

The armchair (zigzag)-edge strips can be thought of as series of finite length zigzag (armchair) chains oriented along the transverse direction of the strip, terminated by hydrogen atoms and stacked edge to edge with each zigzag (armchair) chain containing N carbon atoms and two hydrogen atoms. Considered this way, the primitive translational unit cell of the armchair (zigzag)-edge strips contains two (one) such zigzag (armchair) chains (chain) for a total of $2N$ (N) carbon atoms and 4 (2) hydrogen atoms, as depicted in Figure 1 for the case $N = 7$ ($N = 8$). Note that it is the armchair (zigzag)-edge strips that are more closely related to the zigzag (armchair) SWNTs rather than the other way around because the strips have been named by the bonding pattern along their extended edges,[5] while the SWNTs have been named by the most direct continuous path of C−C bonds around the circumference of the tube.

Even if initially perfect, once physisorbed on a surface, GNSs experience the effects of disorder because of interactions with the substrate. This disorder will ultimately cause localization of their wave functions and hence limit their performance in device applications. Such substrate-induced disorder can be long ranged, arising from substrate charges or other substrate features that produce a potential that changes slowly on a scale of a C−C bond distance, and short ranged, arising from residual interactions with the substrate that cause potential fluctuations varying rapidly on the scale of a C−C bond length. In addition, any strips initially made

* Corresponding author. E-mail: carter.white@nrl.navy.mil.
[†] George Washington University.
[‡] Naval Research Laboratory.

10.1021/nl062132h CCC: $37.00
Published on Web 12/09/2006

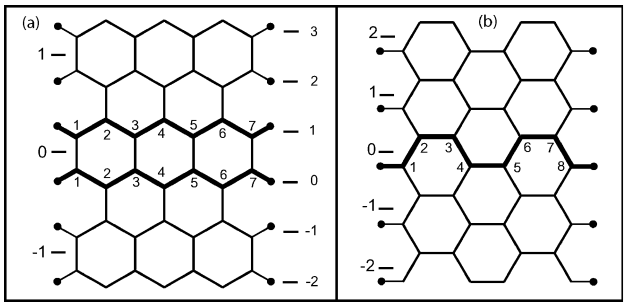

Figure 1. (a) Sample armchair-edge GNS with $N = 7$. Three unit cells are shown numbered at the left edge from -1 to 1. Each unit cell is composed of two zigzag C chains terminated by hydrogen atoms, with the two chains corresponding to the unit cell labeled 0 shown as darkened. (b) Sample zigzag-edge GNS with $N = 8$. Five primitive translational unit cells are shown numbered on the left from -2 to 2. Each unit cell is composed of a single armchair C chain terminated by hydrogens. The chain corresponding to the unit cell labeled 0 is shown as darkened. For both the armchair and zigzag-edge GNSs, $N \geq 2$ and for the zigzag-edge GNSs, N is even.

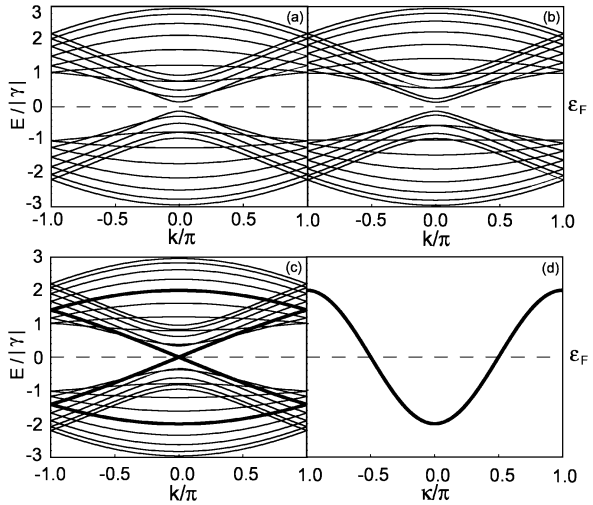

Figure 2. Full-zone band structure of semiconducting [(a) $N = 12$, (b) $N = 13$] and metallic [(c) $N = 14$] armchair-edge GNSs. The bands shown as darkened in (c) have been unfolded to produce the single band in (d), which corresponds to a "unit cell'" one-quarter the actual unit cell.

are likely to have irregular edges that could also affect their performance.

To study the effects of these various types of disorder on the transport properties of GNSs, we adopt the standard tight-binding model described by the Hamiltonian, $\hat{H}_0$, which retains only nearest-neighbor π matrix elements between orthonormal $|p_\pi\rangle$ orbitals (one per carbon atom) oriented normal to the plane of the strip with all diagonal matrix elements fixed at the Fermi level, $\epsilon_F \equiv 0$ eV, and all off-diagonal nonzero matrix elements fixed at $\gamma = -2.7$ eV. Local density functional (LDF) calculations have established that this model provides a good description of the band structure of graphene and metallic and semiconducting SWNTs in the vicinity of ϵ_F.[12] The effects of disorder are then incorporated by adjusting these matrix elements. This model assumes that the strip edges are always terminated by compensating dangling sp^2 hybrids at edge C atoms with H atoms to form strong C−H σ bonds.[5,6] Nearest-neighbor C−H matrix elements associated with these H atoms do not appear explicitly in $\hat{H}_0$ because these σ orbitals (like the sp^2 orbitals used to form strong C−C σ bonds in the strip interior) are symmetric with respect to the nodal plane of the π orbitals and hence decouple from the π conduction bands described by $\hat{H}_0$. Also, because C forms a strong covalent bond with H, the σ and σ^* bands associated with these bonds (like the σ and σ^* bands associated with the C atom in the strip interior) lie far from ϵ_F and hence need not be considered further. In addition, the band structure obtained from $\hat{H}_0$ is in excellent agreement with corresponding LDF results[13] for H-terminated zigzag GNSs in the region of interest near ϵ_F, which shows that any residual shifts in the on-site diagonal matrix elements of $\hat{H}_0$ at the edge C atoms bonded to H can be neglected.

The conductance, G, of a disordered GNS is calculated using a real-space Green function method.[14] In implementing this approach, we assume ideal leads to ensure that the calculated properties arise from the strip and not the contacts. Thus, the left and right leads are modeled by perfect semi-infinite GNSs, which differ only in that one extends to the left and the other to the right. These semi-infinite leads are then connected to one another via a disordered sample GNS with the structure of the leads and their contacts to the sample chosen so that the left-lead-sample-right-lead system is a perfect extended GNS in the absence of sample disorder.

Consider first the armchair-edge GNSs. In the absence of disorder, these strips have properties that are both similar to as well as different from their zigzag SWNT counterparts. First, like the zigzag SWNTs, they can be either metallic or semiconducting, depending respectively on whether or not $N + 1 = 3q$, with q a positive integer,[5,6] as illustrated by Figure 2a−c. Also, like the metallic zigzag SWNTs, the transverse boundary conditions cause all but a few of the bands allowed for the metallic armchair-edge GNSs to be removed from the immediate vicinity of ϵ_F. However, unlike the metallic SWNTs, where the transverse boundary conditions allow two open conduction channels near ϵ_F, the corresponding conditions for the metallic armchair-edge GNSs allow only one. In particular, for the zigzag SWNTs, Born−von Karman boundary conditions allow both sine and cosine solutions around the circumference of the tube, leading to doubly degenerate bands near ϵ_F. However, for the corresponding zigzag-edge strips, Dirichlet boundary conditions require a node at the edges, excluding the cos solutions and leading to a singly degenerate band in the vicinity of ϵ_F. As a consequence, these strips, if ideal, will have a minimum metallic conductance of $2e^2/h$ rather than the $4e^2/h$ found for the metallic zigzag SWNTs.

One might conclude that conduction through the metallic armchair-edge GNSs at low bias would be sensitive to the effects of substrate-induced, long-ranged potential variations because of the small Δk involved in backscattering from the single right-moving to the single left-moving channel near ϵ_F in Figure 2c. This, however, is not the case, as can be seen by using a unitary transformation to unfold the bands shown as darkened in Figure 2c to obtain those of Figure 2d and then noting that potentials varying slowly on the scale

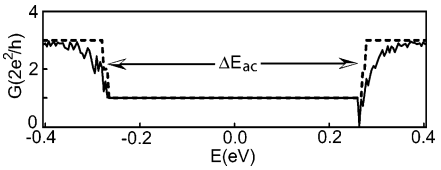

Figure 3. Conductance of a μm long, 6.40 nm ($N = 53$) wide armchair-edge GNS with (solid line) and without (dashed line) disorder introduced[10] by using 3D Gaussian potentials of the form $V(r) = V_0 \exp(-r^2/2\sigma^2)$, with $V_0 = -0.5$ eV and $\sigma = 0.348$ nm, to shift the model diagonal matrix elements. Six such potentials were included, centered at randomly chosen points within the strip, corresponding to a fixed positive substrate charge density of $\sim 10^{11}$ charges/cm^2 appropriate for high-quality SiO_2 substrates. The single-channel window opens by ΔE_{ac} due to transverse confinement.

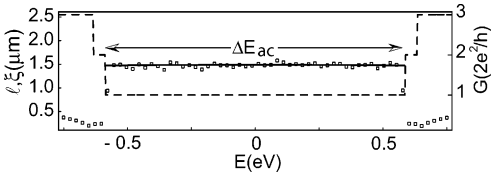

Figure 4. A comparison of ℓ obtained from eq 2 (solid line) to ξ computed from the slope $-\langle \ln[G(L)/g] \rangle_{avg}$ (squares) in the limit of large L. The average is taken over an ensemble of 1000 disordered metallic armchair-edge GNSs with $N = 23$ and diagonal and nonzero off-diagonal matrix elements, each chosen from a rectangular probability distribution of width 0.2 eV centered at their respective ideal values. Also shown in the background is G for the ideal $N = 23$ strip (dashed line).

of a C−C bond distance will be ineffective in causing backscattering because of the phase shift of approximately π involved in this unfolded representation. In contrast, the other π bands that are parabolic cannot be unfolded in this fashion and hence should be sensitive to the effects of long-range disorder. Both expectations are confirmed in Figure 3, where long-range potential fluctuations are seen to have little if any effect on the ideal conductance within the armchair-edge GNS single-channel window,

$$\Delta E_{ac} \cong \frac{2\sqrt{3}\pi}{N+1} |\gamma| \qquad (1)$$

where the transport remains ballistic, but appreciable effect outside this window. This behavior is similar to that found for SWNTs.[9,10]

Although metallic armchair-edge GNSs largely avoid the effects of long-range disorder within the single-channel window, ΔE_{ac}, the conductance of these strips will still be susceptible to elastic backscattering caused by potential fluctuations arising from the substrate that vary on the scale of a C−C bond length. The effects of such residual disorder can be incorporated into the starting model by assuming that the diagonal and nonzero off-diagonal matrix elements are not fixed at their values in the perfect strip but rather are independent random variables with variances σ_ϵ^2 and σ_γ^2, respectively.[8] In the weak scattering limit, the mean free path, ℓ, for carrier backscattering within ΔE_{ac} can then be obtained analytically from the model using Fermi's golden rule and is given by:

$$\ell(E) = \frac{1}{4} \frac{(4\gamma^2 - E^2)}{(4\sigma_\gamma{}^2 + \sigma_\epsilon{}^2)} (N+1) d_0 \qquad (2)$$

where $d_0 \approx 0.142$ nm is the C−C bond length and E the energy measured with respect to ϵ_F. Motion of carriers on the scale of ℓ is expected to be largely ballistic, but for distances larger than ℓ, this single-channel system will quickly enter a localized regime where the resistance increases exponentially with increasing strip length.

The steps leading to eq 2 are lengthy and are outlined as Supporting Information. Note, however, that for a single channel, within the weak scattering limit, $\ell = \xi$, where ξ is one-half the amplitude localization length.[15,16] Also note that, deep within the localization regime, the conductance of the strip behaves as $G(L) = g \exp(-L/\xi)$ with increasing strip length L (ref 16), where $g = 2e^2/h$. Thus, ξ^{-1}, and hence ℓ^{-1}, can be obtained from the slope of the curve $-\langle \ln[G(L)/g] \rangle_{avg}$ for large L, where $\langle\ \rangle_{avg}$ denotes an ensemble average over the disorder.[13] In Figure 4, we compare results for $\ell(E)$ determined in this way to those determined from eq 2. The agreement is excellent over the single-channel window ΔE_{ac}, providing a stringent test of eq 2.

As the transverse size of a normal metallic quantum wire increases, ℓ remains largely fixed for a constant amount of disorder. However, eq 2 shows that, unlike normal wires, metallic armchair-edge strips have ℓs that increase with the width of the wire. This remarkable property arises because the metallic strips, like the SWNTs, have an electronic structure near ϵ_F, which is essentially independent of their width. This allows the single-channel states in wider-width metallic strips to take better advantage of averaging of the short-range potential fluctuations over the width of the strip without having to confront additional states for backscattering. This in turn causes ℓ to increase linearly as wider and wider metallic strips are considered. There are practical limits because the single-channel window, ΔE_{ac}, over which ballistic transport occurs, closes with increasing strip width (see eq 1). However, the relationship between ℓ and strip width together with the large C−C interaction that makes γ^2 large and the observed stability of graphene that makes σ_ϵ^2 and σ_γ^2 small means that metallic armchair-edge GNSs with perfect edges can sustain ballistic transport over micrometers in the presence of short-range disorder while still maintaining a significant ΔE_{ac}. For example, consider a disordered strip where the C−C bond lengths, d, vary independently with equal probability by as much as $\pm 1\%$ from their ideal value. Then eq 2 yields $\ell \cong 9$ μm for a 6.40 nm ($N = 53$) wide metallic armchair-edge GNS because γ will change with d as $\delta\gamma = \alpha\delta d$ with $\alpha \approx 47$eV/nm (ref 8) so that $\sigma_\gamma \approx 0.04$ eV, while eq 1 yields $\Delta E_{ac} \cong 0.54$ eV.

Unfortunately, the exceptional ballistic transport properties of metallic armchair-edge GNSs are easily ruined by irregular edges. Such disorder can be incorporated into the model by eroding the outermost strip edges by randomly removing H−C−C−H groups with a probability P and rebonding the C sp^2 dangling hybrids that result to H atoms. This requires

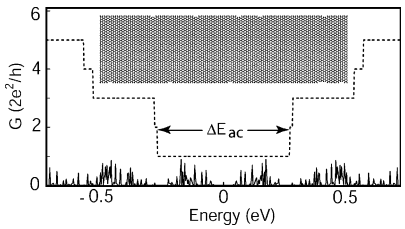

Figure 5. Conductance, G, of a perfect (dashed line) and corresponding edge-disordered (solid line) 1 μm long, 6.40 nm wide ($N = 53$), metallic armchair-edge strip. The *only* form of disorder present in the imperfect armchair-edge strip is a 10% concentration of edge defects described in the text and illustrated for a short segment in the insert.

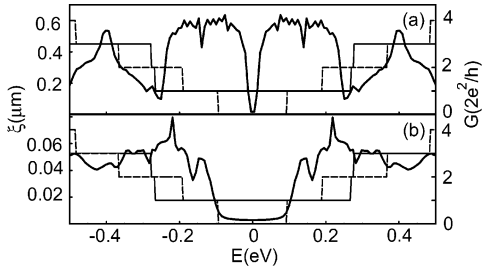

Figure 6. ξ calculated from the slope of $-\langle \ln[G(L)/g] \rangle_{avg}$ at large L for a metallic armchair-edge strip with $N = 53$ for (a) 5% and (b) 50% concentrations of the edge defects described in the text. The ensemble contains 250 realizations of the disorder. Also shown is G for the corresponding ideal metallic (thin solid line) $N = 53$ and semiconducting (dashed line) $N = 52$ strips.

removing pairs of C−C atoms such as labeled by 7's or 1's in Figure 1a and their associated H atoms rather than removing isolated C−H groups. (This constraint arises because, if isolated C−H groups were removed, then the dangling sp^2 C hybrids at the edge cannot be healed by 1-fold coordinated H atoms without severe steric problems.). Figure 5 shows that only a 10% concentration ($P = 0.1$) of these defects destroys the ballistic transport through a 6.4 nm wide ($N = 53$) metallic armchair-edge strip at micron distances. This behavior is further quantified in Figure 6a, where it is seen that even if the concentration of these defects is as low 5%, ξ has been reduced to about 0.6 μm over much of the single-channel window for metallic armchair-edge strips of this width. The dip in ξ around ϵ_F in Figure 6a can be explained in terms of the band structure of the ideal strips. In particular, the right- and left-moving bands in Figure 2c cross because they are decoupled. If the defects are introduced at low concentrations but in a periodic fashion, they couple these bands, converting this crossing to a small avoided crossing. Introducing the same defects randomly also couples these bands, causing backscattering with the small gap appearing in the periodic case now reflected as a dip in ξ. The situation greatly worsens with increasing concentrations of such defects, as shown in Figure 6b. Once again, the relatively small values of ξ around ϵ_F can be explained in terms of the band structure of the ideal strips. In particular, it is understandable that ξ has been limited to about 5 nm in Figure 6b when $|E| < E_0 \cong |\gamma|\pi/\sqrt{3}(N + 1)$ because the strip is now primarily a semiconductor with a gap of $2E_0$ and carriers must tunnel from metallic island to metallic island. However, it is disappointing that ξ has been limited to about 60 nm in regions of energy where the ideal semiconducting and metallic armchair-edge strips both have a single open right-moving channel.

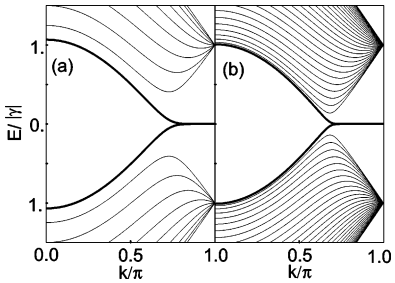

Figure 7. Half-zone model π-band structure near ϵ_F of zigzag GNSs with (a) $N = 20$ and (b) $N = 64$.

Therefore, we find that, because of their narrow widths leading to energetically isolated bands at ϵ_F, armchair-edge GNSs exhibit robust ballistic transport in the presence of substrate-induced disorder. Although different in detail, this behavior is similar to that of metallic SWNTs with similar origins. However, the existence of isolated bands in armchair-edge GNSs over an energy region around ϵ_F comparable to that enjoyed by SWNTs (refs 17−20) requires strips with widths of the order of 10 nm; but then, small amounts of edge disorder ruin the ballistic transport properties of these strips in comparison to SWNTs. Taken together, these results show that if extended armchair-edge GNSs are to have ballistic transport properties similar to seamless metallic SWNTs in the presence of substrate-induced disorder, then a way must be found to make them with near-perfect edges, which could prove a formidable task.

We now turn to the zigzag-edge strips, which we find are not only able to support robust ballistic transport in the presence of substrate-induced disorder but also edge disorder. The unitary transformation used to diagonalize the armchair-edge GNS Hamiltonian does not help for the zigzag-edge GNSs (preventing, e.g., derivation of an expression corresponding to eq 2), so we proceed numerically. In the absence of any disorder, these strips all have similar, although not identical, band structures within a single-channel window, which opens around ϵ_F by $\Delta E_{zz} \approx 5.3$ eV·nm/W, due to the narrow strip width, W. As before, it is within this single-channel window that robust ballistic transport can occur. The flat band region seen in Figure 7 is known to arise from states localized near the strip edges.[5,6] If the strip were infinitely wide, this flat band region would extend exactly from $2\pi/3$ to π, but because W is finite, states on opposite edges interact weakly, making these bands truly degenerate only at the zone boundary. For $|k| < 2\pi/3$, the bands within ΔE_{zz} are closely related to those[21] of corresponding armchair SWNTs.

In the ideal zigzag-edge GNSs, the relatively flat bands seen in Figure 7 will produce a peak in the density of states over a narrow energy range ΔE_p, with carriers at these energies primarily confined to the strip edges. However, if carriers are injected into states outside this narrow range but still within the single-channel window, ΔE_{zz}, then they avoid

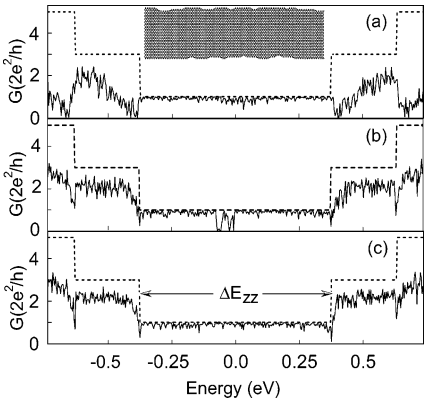

Figure 8. Conductance of a zigzag-edge GNS 1 μm long and 6.7 nm ($N = 64$) wide in the presence of (a) edge disorder modeled by randomly removing edge C atoms up to four layers deep on both sides and rebonding the new edges to hydrogens, as depicted for a short segment in the insert; as with the armchair-edge strips, C atoms are always removed in such a way that any dangling sp^2 hybrids that result can be compensated by H atoms without steric problems. (b) Long-range disorder modeled by introducing the same six Gaussian potentials as used in Figure 3 arranged randomly within the strip, and (c) short-range disorder modeled by adding to each nearest-neighbor matrix element, γ, a random component which allows the C−C bond lengths to vary independently with equal probability by as much as ±1% from their ideal values assuming an electron−phonon coupling constant of 47 eV/nm.

the edges, leading to the possibility that for such energies, these strips could resist the effects of edge disorder. This is confirmed in Figure 8a. The results of Figure 8a are in marked contrast to those of Figure 5, where less irregular edges are found to ruin ballistic transport at μm distances throughout the single-channel window for a similar width armchair-edged strip. Although visually the strip edges in the insert of Figure 8a are a good deal more irregular than those shown in the insert of Figure 5, these differences can be further specified by noting that in Figure 5, only the outermost layer has been eroded at each edge with a concentration of C atoms removed of only 10%. On the other hand, in Figure 8a, up to four layers have been eroded from each edge with a concentration of C atoms removed (ratio of number of carbon atoms removed from an edge to the total number of C atoms in the outermost four layers) of about 50%. In Figure 8a, the edges are eroded randomly up to four layers deep so that each edge varies up to about 6% of the strip width. For zigzag-edge GNSs of this width with this degree of edge erosion, we find that ξ is too long to for us to compute. However, for a greater degree of edge erosion, ξ shortens to the point that we have found that if up to eight layers are randomly eroded from each edge, then ξ calculated for several points within ΔE_{zz} but outside ΔE_p using an ensemble of 250 strips is around 7 μm. We have not attempted to continue the process of zigzag-edge erosion beyond eight layers because the algorithm we have used becomes more complex the deeper the erosion (this algorithm is included as Supporting Information). However, wider width zigzag-edge GNSs should be able to tolerate even a greater degree of edge disorder but at the expense of narrowing the single-channel window.

The zigzag-edge GNSs should also resist the effects of substrate-induced disorder outside ΔE_p but inside ΔE_{zz}. First, potentials that fluctuate slowly on a scale of d_0 should have little effect on the conductance at these energies because of the large Δk (see Figure 7) required for backscattering. This is confirmed by Figure 8b. Note that the deep dips in the conductance a bit below zero in Figure 8b indicate that the edge states tend to become localized down the strip in the presence of fixed positive substrate charges modeled following ref 10. These dips occur below ϵ_F because the potentials are attractive. Also, the zigzag-edge strips, for the same reasons as armchair-edge GNSs, will have ℓ s that increase with increasing W in the presence of short-range disorder, leading to values of ℓ comparable to those obtained from eq 2 for similar width armchair-edge GNSs consistent with Figure 8c. In addition, note that the results are not changed significantly within ΔE_{zz} when all three types of disorder are simultaneously present in the strip. Therefore, these zigzag-edge strips can exhibit robust ballistic conductance at micron distances not only in the presence of edge disorder but also in the presence of both long- and short-range substrate-induced disorder.

The striking differences between Figures 5 and 8a can be understood qualitatively in terms of the ideal strips. In particular, ideal armchair-edge GNSs have states within ΔE_{ac} extending to the strip edges that are sensitive to small changes in the edge boundary conditions; e.g., these strips are either metallic or semiconducting depending respectively on whether or not $N + 1 = 3q$, with q a positive integer (see Figure 2). Therefore, disordering their edges introduces a random mixture of transverse boundary conditions that destroys their ballistic conductance within ΔE_{ac} at micron distances. On the other hand, ideal zigzag-edge GNSs all have similar band structures (see Figure 7), with wavefunctions corresponding to states within ΔE_{zz} but outside ΔE_p that are not much affected by similar changes in the strip width. This allows the strip edges to be varied without drastic changes to these wavefunctions because of the existence of protective, essentially orthogonal edge states. Therefore, states within ΔE_{zz} but outside ΔE_p are a lot less sensitive to the effects of edge disorder, leading to a more robust conductance. The edge states are more affected by edge disorder, but this turns out to be less than might be anticipated, as can be seen by examining G close to ϵ_F in Figure 8a.

Therefore, we have shown that both zigzag and metallic armchair-edge GNSs with ideal hydrogen-terminated edges exhibit outstanding ballistic transport properties in the presence of substrate-induced disorder because of transverse confinement, leading to energetically isolated bands in the neighborhood of ϵ_F. Although different in detail, this behavior is similar to that of SWNTs and has similar origins. However, GNSs differ fundamentally from seamless SWNTs because of the existence of edges, and weakly disordering these edges ruins the ballistic transport properties of armchair-edge GNSs in comparison to SWNTs. On the other hand, states localized along the edges of zigzag-edge GNSs (absent in the armchair-edge strips) protect the remaining states within the single-channel window, leading to ballistic transport properties that

can be comparable to SWNTs in the presence of edge disorder. We do not expect these conclusions to be significantly altered in more refined treatments. For example, the ideal metallic armchair-edge strips will exhibit a small gap if longer range interactions are taken into account, but this gap will diminish with increasing strip width. Also, for the zigzag-edge strips, if electron−electron interactions are included in the model, then the edges could become ferromagnetic, but in this instance, a portion of the ballistic window should remain.

At low bias, transport in graphene will be isotropic. However, the results reported in Figures 5 and 8a show that metallic armchair- and zigzag-edge GNSs with widths around 6.5 nm and lengths of 1 μm cut from graphene have much different transport properties due to disordered edges. One might expect that significant differences in the conductance between the two strip types will be largely confined to the single-channel window, which is roughly equal for both the armchair- and zigzag-edge strips and is inversely proportional to the strip width. However, the results shown in Figures 5 and 8a show that, for these samples, this is not the case. In particular, these results show that, not only is the conductance within the single-channel windows of the armchair- and zigzag-edge strips affected much differently by edge disorder, but also these differences extend into the multichannel diffusive regime outside these windows. Indeed, we have found that, for these strips, these differences extend an eV or so into this multichannel region, with the conductance of the zigzag-edge strip generally more resistant to edge disorder. We have also found for armchair-edge strips of this width that this is true regardless of whether we start with a semiconducting or metallic armchair-edge strip. Thus, we suggest that for armchair- and zigzag-edge strips (with similar widths, lengths, and edge disorder) the conductance of zigzag-edge strips will more rapidly approach that of the corresponding ideal strip outside the single-channel window with increasing strip width. We further conjecture that differences in the conductance between these two strip types could be observable for strips an order of magnitude wider than we have treated if they are long enough because the conductance of the predominately armchair-edge strips should more rapidly degrade within the multichannel regime with increasing length due to edge disorder.

If the strip axis is oriented with respect to the graphene sheet along a direction intermediate between armchair and zigzag directions, then its edges will exhibit a mixture of armchair and zigzag edges.[6] If we define these strips following ref 6, then their edges will be periodic but can exhibit long repeat distances, leading to large translational unit cells. These long unit cells make the conductance of such strips difficult to calculate assuming perfect contacts. However, the results we have obtained in the limiting zigzag- and armchair-edge cases allow us to conjecture somewhat about the behavior of these intermediate cases. If the angle θ between the strip axis and the zigzag direction is small, the ideal strip will have predominately zigzag edges with only occasional armchair-edge steps. These steps, however, will be similar to ones we have already included in disordering the zigzag-edge strip edges and should be largely masked by similar edge disorder. Thus, we expect that the conductance of this edge-disordered off-axis strip, although perhaps not quite as good, will remain close to an edge-disordered zigzag-edge strip of the same width and length. If θ is close to $\pi/6$, the ideal strip should divide into relatively long metallic and semiconducting segments. However, we expect each segment to be sensitive to edge disorder, as in the case of perfect armchair-edge GNSs. Thus, we expect that the conductance of this edge-disordered off-axis strip, although perhaps not quite as good, will remain close to an edge-disordered armchair-edge strip of the same width and length. For an arbitrary θ, we can only conjecture that the conductance will degrade as the ratio of armchair to zigzag-edge sites increases, with this ratio affected both by θ and the edge disorder.

We have focused herein on sources of disorder that are going to be difficult to remove even with high-quality samples on high-quality substrates. Thus, we have concentrated on the effects of substrate-induced and edge disorder. In analogy with SWNTs,[22] other types of disorder could prove important in tailoring the properties of these strips for specific transport applications, e.g., high concentrations of N or B impurities introduced by doping[23] or vacancies or divacancies introduced by ion bombardment.[24] We have also assumed that the strip edges are hydrogen-terminated, but using different chemical species or groups could provide an additional avenue for tailoring the strip properties. The existence of edges makes it difficult to pin down the transport properties of these strips in comparison to SWNTs, but these edges also provide an opportunity to adjust the strip properties for particular applications. For example, our results imply that hydrogen-terminated zigzag-edge GNSs are better initial synthetic targets for ballistic device applications. On the other hand, the sensitivity of hydrogen-terminated armchair-edge strips to edge disorder might ultimately make them useful as sensors.

Acknowledgment. We thank John Mintmire, Philip Kim, and James Murday for discussions. This work was supported by ONR both directly and through the Naval Research Laboratory.

Supporting Information Available: Expanded view of table of contents graphic with associated figure caption; outline of steps leading to eq 2; description of zigzag-edge disordering algorithm. This material is available free of charge via the Internet at http://pubs.acs.org.

References

(1) Novoselov, K. S.; Jiang, D.; Schedin, F.; Booth, T. J.; Khotkevich, V. V.; Morozov, S. V.; Geim, A. K. *Proc. Natl. Acad. Sci. U.S.A.* **2005**, *102*, 10451.
(2) Novoselov, K. S.; Geim, A. K.; Morozov, S. V.; Jiang, D.; Katsnelson, M. I.; Grigorieva, I. V.; Dubonos, S. V.; Firsov, A. A. *Nature* **2005**, *438*, 197.
(3) Zhang, Y.; Tan, Y.-W.; Stormer, H. L.; Kim, P. *Nature* **2005**, *438*, 201.
(4) Berger, C.; Song, Z.; Li, X.; Wu, X.; Brown, N.; Naud, C.; Mayou, D.; Li, T.; Hass, J.; Marchenkov, A. N.; Conrad, E. H.; First, P. N.; de Heer, W. A. *Science* **2006**, *312*, 1191.

(5) Fujita, M.; Wakabayashi, K.; Nakada, K.; Kusakabe, K. *J. Phys. Soc. Jpn.* **1996**, *65*, 1920.
(6) Nakada, K.; Fujita, M.; Dresselhaus, G.; Dresselhaus, M. S. *Phys. Rev. B* **1996**, *54*, 17954.
(7) Tans, S. J.; Devoret, M. H.; Dai, H.; Thess, A.; Smalley, R. E.; Geerligs, L. J.; Dekker: C. *Nature* **1997**, *386*, 474.
(8) White, C. T.; Todorov, T. N.; *Nature* **1998**, *393*, 240; White, C. T.; Todorov, T. N. *Nature* **2001**, *411*, 649.
(9) Ando, T; Nakanishi, T. *J. Phys. Soc. Jpn.* **1998**, *67*, 1704; Ando, T.; Nakanishi, T.; Saito, R. *J. Phys. Soc. Jpn.* **1998**, *67*, 2857.
(10) McEuen, P. L.; Bockrath, M.; Cobden, D. H.; Yoon, Y.-G.; Louie, S. G. *Phys. Rev. Lett.* **1999**, *83*, 5098.
(11) Liang, W.; Bockrath, M.; Bozovic, D.; Hafner, J. H.; Tinkham, M.; Park, H. *Nature* **2001**, *411*, 665.
(12) For a recent review, see White, C. T.; Mintmire, J. W. *J. Phys. Chem. B* **2005**, *109*, 52.
(13) Miyamoto, Y.; Nakada, K.; Fujita, M. *Phys. Rev. B* **1999**, *59*, 9858.
(14) Todorov, T. N. *Phys. Rev. B* **1996**, *54*, 5801.
(15) Thouless, D. J. *J. Phys. C: Solid State Phys.* **1973**, *6*, L49.
(16) Johnson, R; Kunz, H. *J. Phys. C: Solid State Phys.* **1983**, *16*, 3895.
(17) Wildöer, J. W. G.; Venema, L. C.; Rinzler, A. G.; Smalley, R. E.; Dekker, C. *Nature* **1998**, *391*, 59.
(18) Odom, T. W.; Huang, J.-L.; Kim, P.; Lieber, C. M. *Nature* **1998**, *391*, 62.
(19) White, C. T.; Mintmire, J. W. *Nature* **1998**, *394*, 29; Mintmire, J. W.; White, C. T. *Phys. Rev. Lett.* **1998**, *81*, 2506.
(20) Charlier, J.-C.; Lambin, Ph. *Phys. Rev. B* **1998**, *57*, R15037.
(21) Mintmire, J. W.; Dunlap, B. I.; White, C. T. *Phys. Rev. Lett.* **1992**, *68*, 631.
(22) Charlier, J.-C. *Acc. Chem. Res.* **2002**, *35*, 1063.
(23) Latil, S.; Roche, S.; Mayour, D.; Charlier, J.-C. *Phys. Rev. Lett.* **2004**, *92*, 256805.
(24) Biel, B.; García-Vidal, F. J.; Rubio, A.; Flores, F. *Phys. Rev. Lett.* **2005**, *95*, 266801.

NL062132H